



Hydrogeophysical and structural investigation using VES and TDEM data: A case study at El-Nubariya–Wadi El-Natrun area, west Nile Delta, Egypt



Ismael M. Ibraheem^a, Gad M. El-Qady^{b,*}, Ahmed ElGalladi^c

^a *The General Establishment of Geology and Mineral Resources, Ministry of Petroleum and Mineral Resources, 7645, Syria*

^b *National Research Institute of Astronomy and Geophysics, Helwan, Egypt*

^c *Faculty of Science, Mansoura University, Egypt*

Received 19 February 2016; revised 22 April 2016; accepted 22 April 2016

Available online 13 May 2016

KEYWORDS

Dc resistivity;
TEM;
Groundwater;
El-Nubariya;
Wadi El-Natrun;
Egypt

Abstract The geoelectric survey includes 93 Vertical Electric Soundings (VES) and 26 TEM stations were conducted to delineate the subsurface structures and hydrogeological regime of El-Nubariya–Wadi El-Natrun area. The VESes AB/2 was varying from 1 up to 700 m in successive steps, while TEM stations were measured using coincident loop of 50 m side length.

The interpretation of the geoelectrical data shows that the depth to the main aquifer ranges from 6 m at the northern part near the Nubariya city to about 90 m at the southern parts where it increases to the south and southeast directions. Generally the aquifer system in the area can be divided into Pleistocene and Pliocene aquifers. The Pleistocene aquifer is the shallower aquifer in the area and it consists almost of gravelly to clayey sand deposits. The Pliocene aquifer is the main aquifer where it is composed of sand to gravelly sand deposits.

Depending on the results of the geoelectric prospecting represented by the true resistivity map, we can infer the quality of the groundwater. A brackish groundwater can be found at the northern and northeastern parts of the study area at shallow depths whereas relatively fresh water can be detected at the southern and southeastern parts around Wadi El Natrun city at deep depths.

* Corresponding author.

E-mail addresses: ismael.geo@gmail.com (I.M. Ibraheem), gadosan@nriag.sci.eg (G.M. El-Qady).

Peer review under responsibility of National Research Institute of Astronomy and Geophysics.



Production and hosting by Elsevier

<http://dx.doi.org/10.1016/j.nrjag.2016.04.004>

2090-9977 © 2016 Production and hosting by Elsevier B.V. on behalf of National Research Institute of Astronomy and Geophysics. This is an open access article under the CC BY-NC-ND license (<http://creativecommons.org/licenses/by-nc-nd/4.0/>).

The area under consideration is affected by a group of normal faults that divided the investigated area into five main divisions, northern, eastern, western, southern and central divisions. The inferred faults from the geoelectric sections are traced and collected to construct a structure map. It is worth to mention that Wadi El Natrun and its lakes are structurally controlled by faulting systems trending NW direction.

© 2016 Production and hosting by Elsevier B.V. on behalf of National Research Institute of Astronomy and Geophysics. This is an open access article under the CC BY-NC-ND license (<http://creativecommons.org/licenses/by-nc-nd/4.0/>).

1. Introduction

Electrical resistivity method is, generally, considered to be the most promising and most suitable method for ground water prospecting. This is based on the concept of determination of the subsurface, which can yield useful information on the structure, composition and content of buried formation (Keller, 1967).

A great attention is paid by different Egyptian Authorities for the establishment of the new settlements and land reclamation projects to overcome the over population crisis and to construct new agricultural areas. In this respect, priorities are given to west Nile Delta area, which is considered as a promising region due to its distinct location, mild weather, easy accessibility and the availability of water supplies. Accordingly, new desert settlements are established e.g. South El Tahrir, El

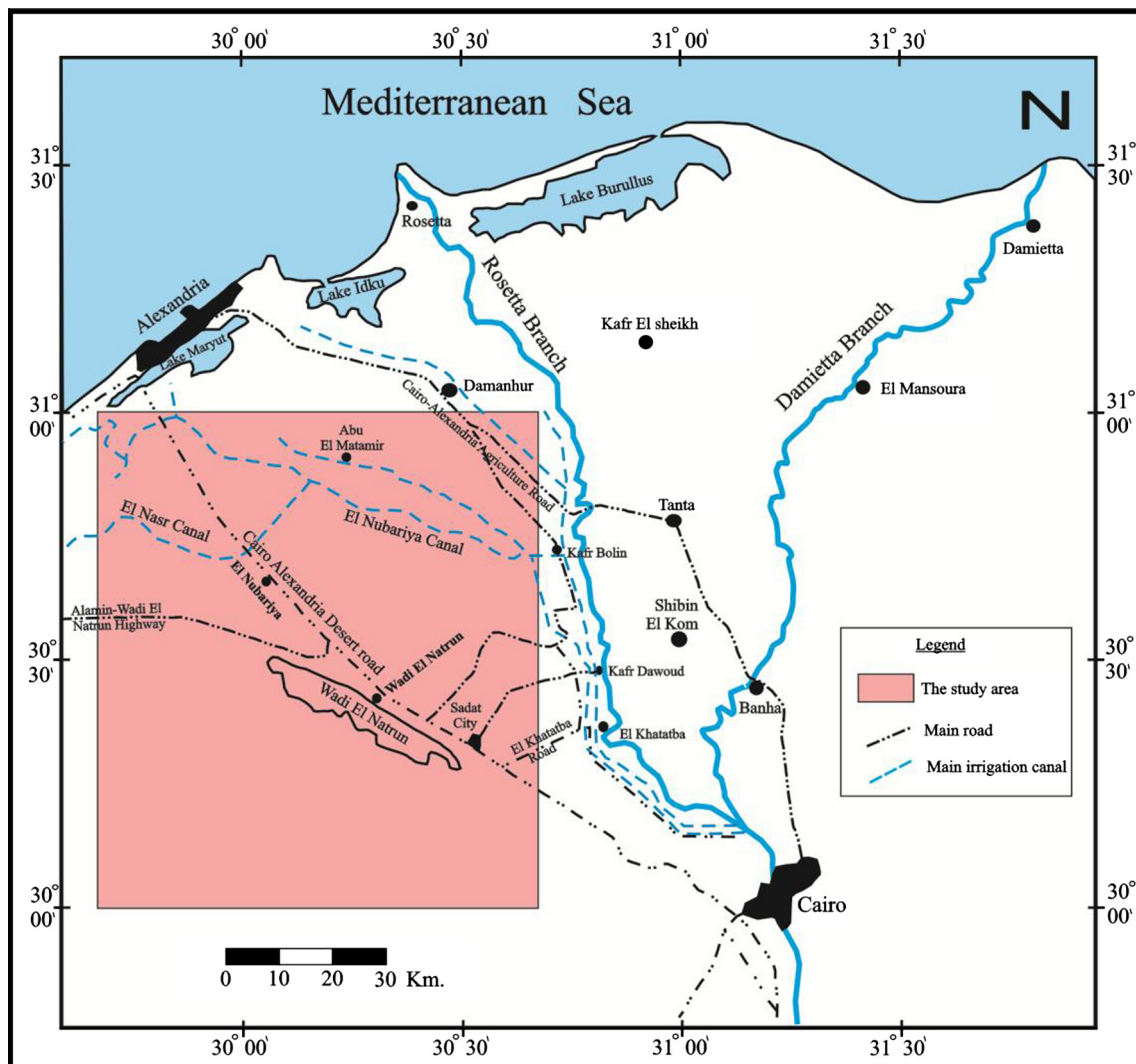


Figure 1 Location map for the study area and its surroundings.

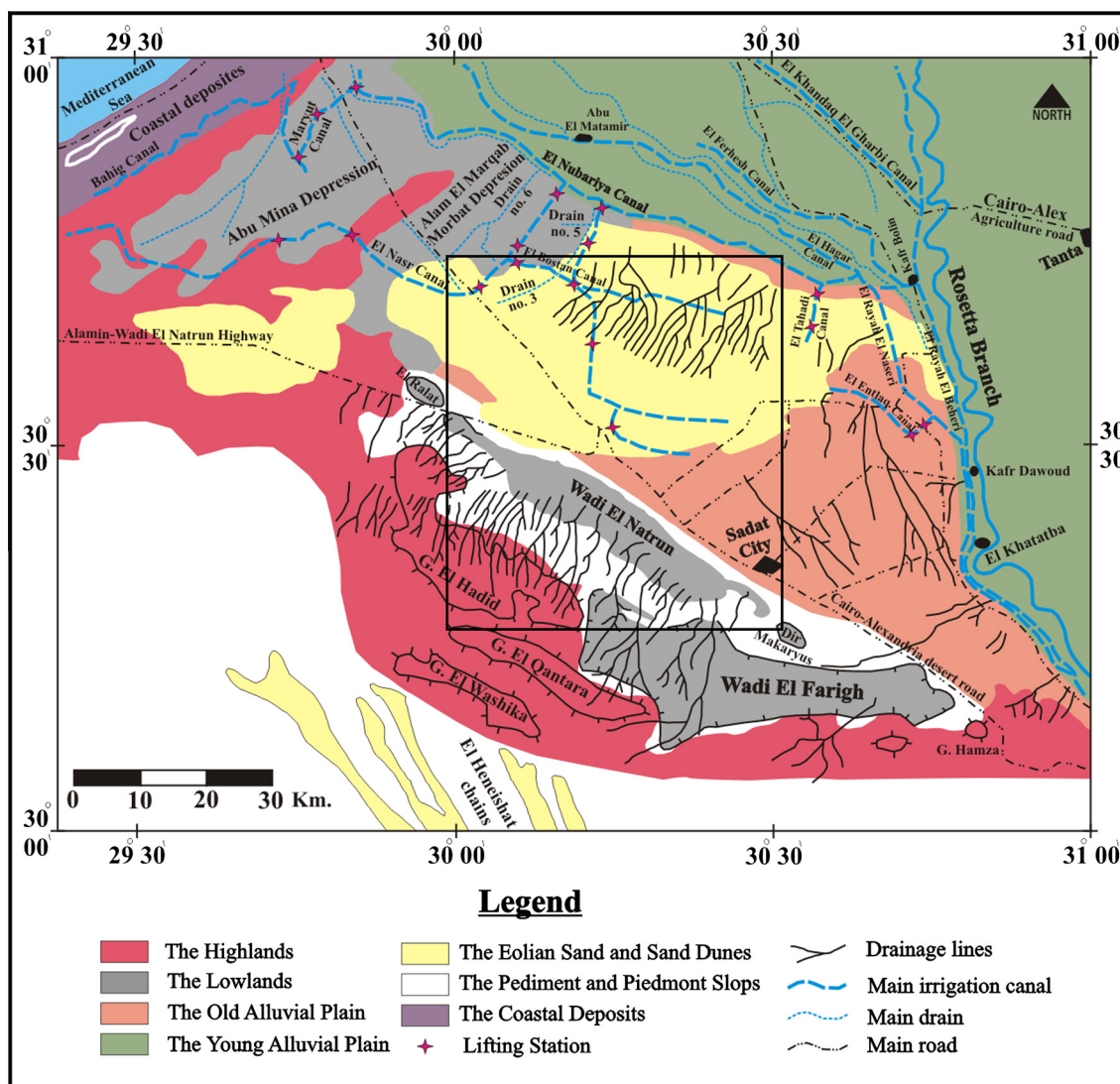


Figure 2 Detailed geomorphologic map characterized landforms of west Nile Delta area (reproduced after Embaby, 2003).

Sadat city, El Nubariya and El Bustan pilot areas, in addition to many villages and farms.

For this purposes, the present research is planned in order to address the structural setting and evaluate the hydrogeological regime in the area of El Nubaryia-Wadi El-Natronun using geoelectrical methods.

The area under investigation (Fig. 1) is located to the west of Nile Delta on both sides of the Cairo-Alexandria desert road, between latitudes $30^{\circ}17'$ and $30^{\circ}42'N$, and longitudes $30^{\circ}00'$ and $30^{\circ}30'E$. It covers an area of about 1250 km². Wadi El Natrun depression nearly occupies the southern part of the area. The main cities in the study area are El Nubariya, Wadi El Natrun, and Sadat City. It is accessible from Cairo, Alexandria, Northwestern Coastal zone and central part of the Nile Delta by good roads system.

Generally, the present work is essentially concerned with the interpretation of the available geoelectrical data (VES and TDEM stations) in order to determine the groundwater

aquifers and the structural setting in the area under investigations.

2. Geological context

2.1. Topography and geomorphology

The western Nile Delta fringe is generally characterized by slightly undulating topography and higher land comparing with those of cultivated part of Nile Delta where the highest point is found in Qaret El Haddadein plateau where its ground elevation attains +23 m above mean sea level and the lowest point is located at Wadi El Natrun with approximately elevation of -23 m below mean sea level.

Generally, the geomorphologic studies of the area west of the Nile Delta were addressed by many authors such as Sandford and Arkell (1939), Said (1962), Shata and El

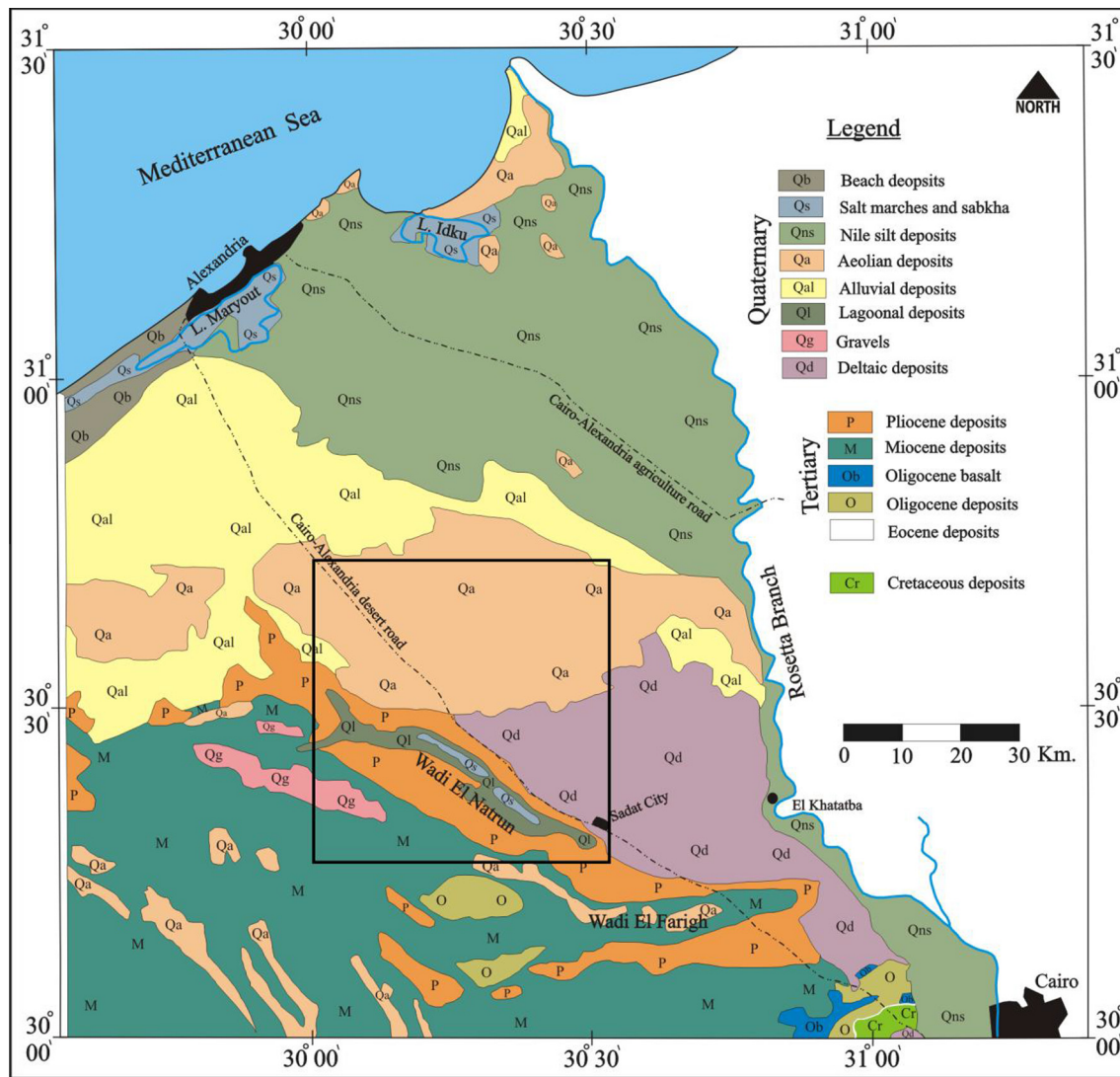


Figure 3 Geological map of the area west of Nile Delta (reproduced after CONCO, 1987).

Fayoumi (1967), Abu El-Izz (1971), El Shazly et al. (1975), and Embaby (2003). Most of those Authors classified the western fringe of the Nile Delta into six significant landforms. Embaby (2003) suggested a new detailed geomorphologic map (Fig. 2) where the west Nile Delta can be classified into the following geomorphologic units: The high lands 2 – The lowland 3 – The pediment and piedmont slops 4 – The old alluvial plain 5 – The young alluvial plain 6 – The eolian sand and sand dunes and 7 – The drainage system.

2.2. Surface and subsurface geology

The geology of west Nile Delta is discussed by several authors such as Sandford and Arkell (1939), Shata (1953, 1955, 1959), Said (1962), Shata et al. (1970, 1978). The exposed rocks in the study area (Fig. 3) belong to Cenozoic (Tertiary and Quaternary).

Neogene sediments are generally dominating the southern and western parts at El Ralat, Wadi El Natrun, and Wadi El Farigh depressions as well as at El Washika, Dahr El Tashasha and Gebel El Hadid ridges. They composed of sand and sandstone with clay and limestone intercalations. The Quaternary sediments are mainly clastic with essential sand facies and occasional gravel and clay intercalations.

In the subsurface, the sedimentary rocks overlying the basement complex have a thickness of about 4000 m, as recorded from Sahara Wadi El Natrun test well. The sedimentary rock succession starts from base by Triassic rocks resting on the basement rocks and ends at top with recent deposits of the Quaternary.

2.3. Structure and tectonics

Generally, the structural setting and tectonics of the Egyptian territory, including the area under investigation, had been

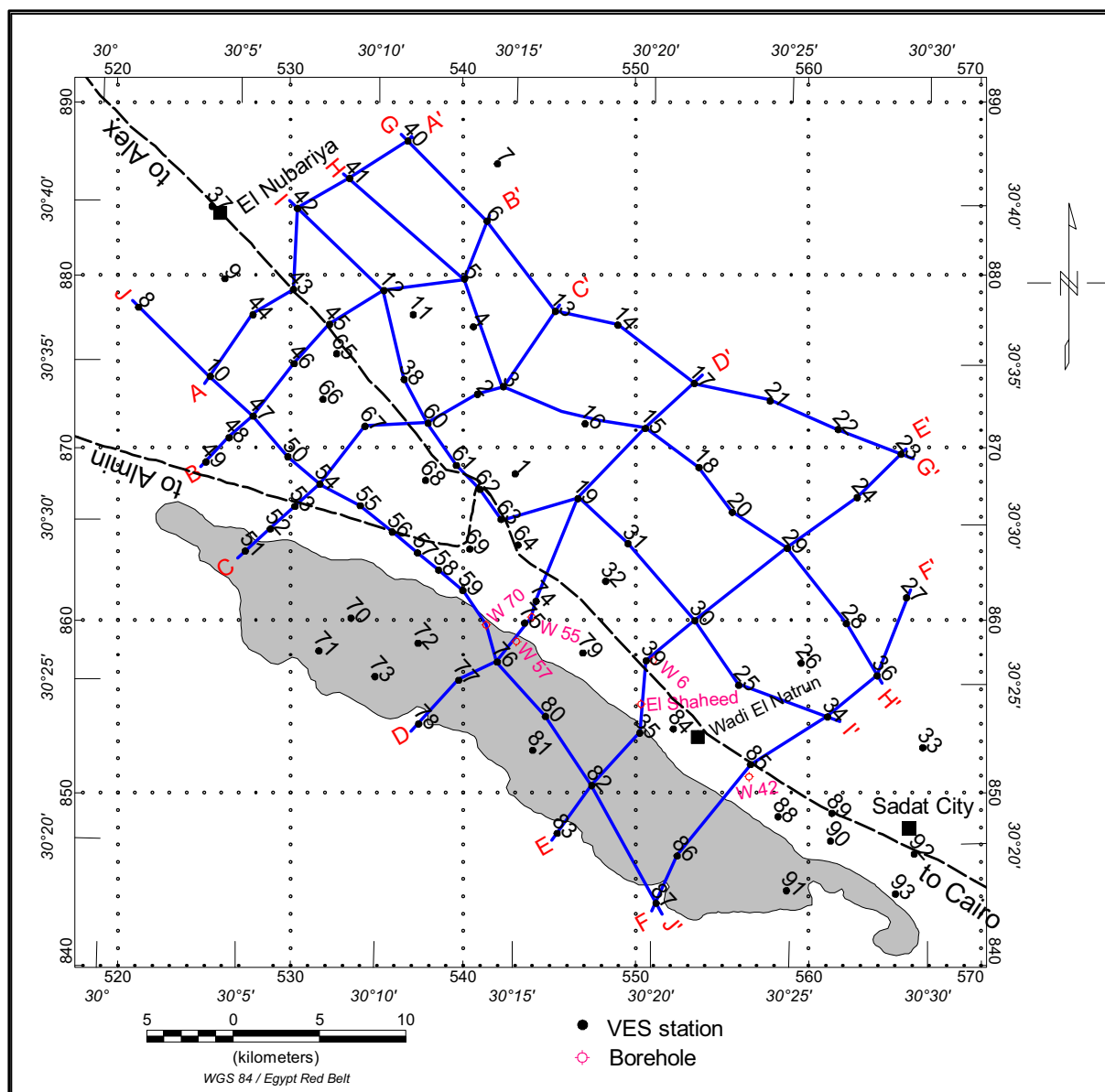


Figure 4 Location map of the VES stations, boreholes and selected profiles.

dealt with many authors such as Shukri (1954), Yalouze and Knetsch (1954), Said (1962), Youssef (1968), Idris (1970), Moody (1973), El Shazly et al. (1975), El Shazly (1977), Riad et al. (1981), Meshref (1982), Ahmed and Hassaneen (1985), Tealeb and Abdel Rahman (1985), Abu El Ata (1988), ElGalladi et al. (2009) and others.

Meshref (1982) suggested that, Northern Egypt was affected by three tectonic events. The oldest resulted in NW or WNW trending structures, which was followed by another event that resulted in ENE (Syrian arc) trending structures. The third tectonic event resulted in the E–W, NW (Suez) and NNE (Aqaba) trending structures.

Structurally, the study area is located within the unstable shelf of northern parts of the Western Desert and is mainly

affected by folds, faults, unconformities, and basaltic intrusions. These structural elements are the most important factors influencing the groundwater conditions in the area.

3. Hydrogeological context

Many researchers have investigated the hydrogeology of the area west of Nile Delta among them are as follows: Hefny et al. (1991), Sallouma and Gomaa (1997), Embaby (2003), Khalil et al. (2014), and Massoud et al. (2014).

Hydrogeologically, the groundwater in the study area is mainly controlled by the geological conditions including lithology, topography and structures. The main water-bearing

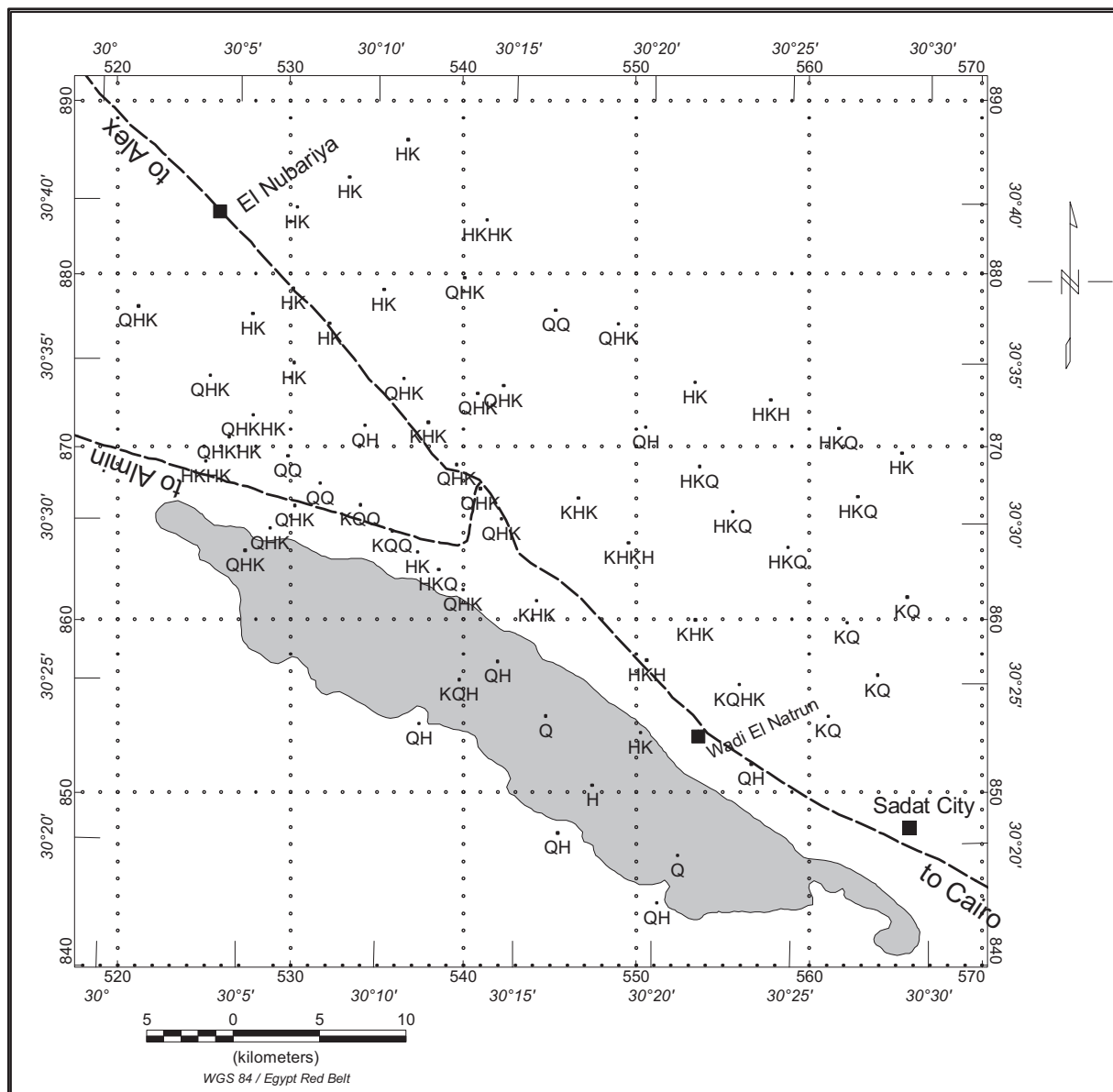


Figure 5 Distribution of the curve types in the study area.

formations belong to Quaternary (Recent and Pleistocene) and Neogene (Pliocene and Miocene).

The surface water system (Fig. 1) in the area under investigation and its vicinities is mainly as follows: Rosetta branch, El Rayah El Beheri, El Rayah El Naseri, the artificial canals and drains, salts lakes and springs. This system is subjected to evaporation, rainfall and infiltration to the groundwater aquifers. The salt lakes get their water from two sources, the springs found in the bottom of Wadi El Natrun and the seepage into lakes from their sides as they are located in low land.

4. Geophysical data

4.1. Vertical Electrical Sounding (VES) survey

To achieve the main goals of this investigation a total of 93 Vertical Electric Soundings (VES) (Fig. 4) were carried out

in the study area and represented by two data sets. The first one is obtained from a previous work of [Abd El-Gawad and Ammar \(2004\)](#) in the area of Wadi El Natrun (VESes 65-93). The second is acquired in a field work (VESes 1-64) by the author himself (Fig. 4). The field measurements were carried out using direct current resistivity meter called McOhm of OYO Corporation, using Schlumberger array with AB/2 ranging from 1.5 m to 700 m in successive steps. In addition to the geoelectric data, a lithology for many boreholes in the study area was collected from many sources.

4.2. Interpretation of VES data

The aerial distribution of the field curve types was constructed as in Fig. 5. We can notice that the curve type QHK is predominant in the western part of the study area whereas the curve type HK characterizes the northern part of the area. Also,

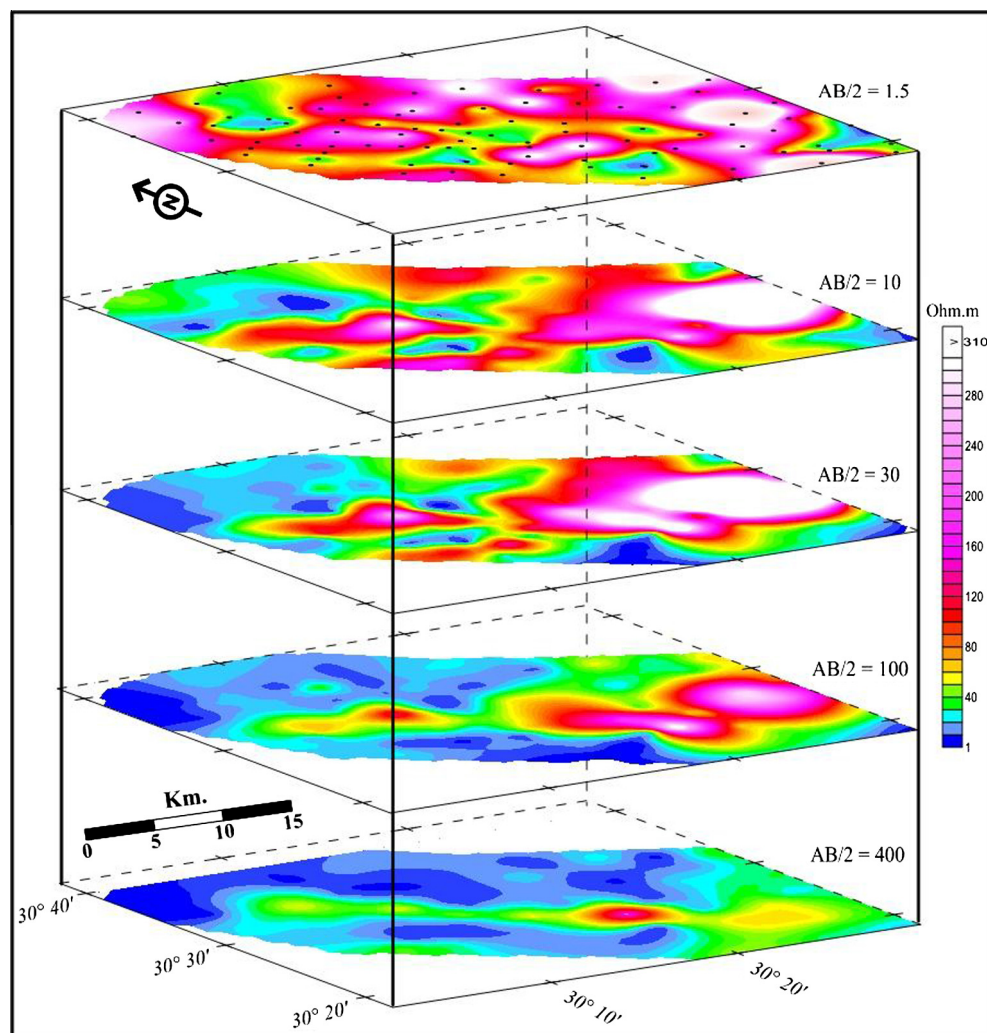


Figure 6 Iso-apparent resistivity map at $AB/2 = 1.5, 10, 30, 100$ and 400 m.

the eastern portion of the area is dominating by KQ and HKQ curve types. Added, the southern part of the area can be constituted by the QH curve type. Finally KHK curve type characterizes the central part of the investigated area. As a result of curve type inspection, we can conclude that the area under consideration may be affected by a group of normal faults that divided the investigated area into five main divisions, which are northern, eastern, western, southern and central divisions.

The Iso-apparent resistivity contour maps are constructed for different electrode spacing to illustrate the resistivity distribution at a successive levels penetrated by the artificial electric current. Each map is prepared for a given electrode separation $AB/2$, to illustrate the geological conditions prevailing within a horizon approximately parallel to the ground surface.

Five iso-apparent resistivity contour maps (Fig. 6) are selected for the electrode separations ($AB/2$: 1.5, 10, 30, 100, and 400 m). From the inspection of the maps we can conclude the following remarks:

1. The surface layer shows variable resistivity values due to lithology heterogeneities and dryness and wetness conditions of the silt, sand and gravel that covers the surface of the study area.
2. The conspicuous lateral variations of the iso-apparent resistivities indicate comparable lateral changes in the encountered types of rocks.
3. The resistivity values generally begin with high values for the smaller depth of penetration, and then decrease gradually by increasing the depth.
4. The eastern region is characterized by high values and may be represented by sand and gravels. Besides, it could be deduced that, the areas located at the northern and western parts (of moderated resistivity values) are saturated with shallow groundwater. Added, the low resistivity values at the area around the lakes of Wadi El Natrun may be affected by the salt water comes from the lakes or it may be represented by clay deposits.

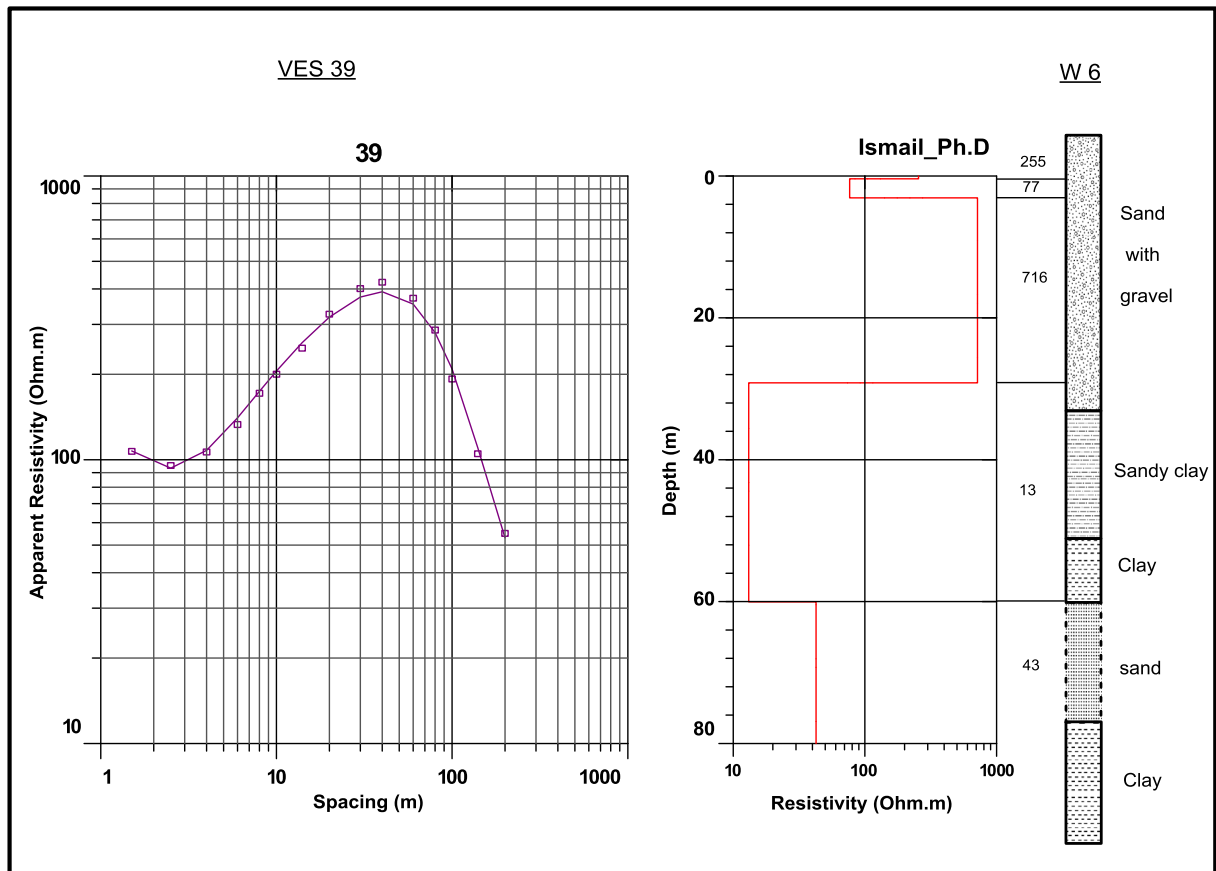


Figure 7 Lithology log of well 6 and its corresponding interpreted geoelectric model.

One-dimensional resistivity inversion was carried out using the software IX1D (IX1D v3 Instruction Manual, 2008) which in this case solves the inversion using a Ridge Regression method (Inman, 1975).

The resistivity values of the VESes were constrained using the drilled boreholes nearby and were correlated with the lithology of those boreholes. Fig. 7 is a good example for the correlation procedure where the VES 39 is correlated with the borehole W6. The geoelectric model shows slight difference from the lithological section.

During the quantitative interpretation, all available data were used to construct the initial model. The VESes carried out in this area was used to construct 10 geoelectric cross sections. Six cross sections are oriented nearly NE–SW and four cross sections are directed mostly NW–SE. Six geoelectric cross sections are selected and shown (Figs. 8–12).

The inspection of the geoelectric cross sections shows that the area of study is divided into five geoelectric units as the following:

- The first geoelectric unit is characterized by relatively very low to very high electric resistivity values ranged between $4 \Omega \text{ m}$ at VES 35 and $4031 \Omega \text{ m}$ at VES 30. The great differences in resistivity of this layer reflect the inhomogeneity of

lithology, which corresponds to sand, silt, clay, gravel and gravelly sand. The low resistivity values are recorded in the area of salt marshes where a layer of salt covers the surface.

- The second geoelectric layer shows relatively low resistivity values ranged between $2 \Omega \text{ m}$ and $15 \Omega \text{ m}$, which corresponds to clay deposits. The thickness of this layer is ranging between 1 m at VES 40 and 44 m at VES 78. A lens of clayey sand, sand and gravelly sand corresponds to low to high resistivity values $14\text{--}421 \Omega \text{ m}$ are found above this clay layer. This lens appears in cross sections C–C' and D–D'.
- Relatively moderate electric resistivity values ranged between $15 \Omega \text{ m}$ (VES 12) and $75 \Omega \text{ m}$ (VES 53) characterizing the third geoelectric unit constituting the main aquifer in the area. The thickness of this unit is ranged between 13 m (VES 6) and 83 m (VES 53) which corresponds to sand deposits.
- The fourth geoelectric unit is characterized by relatively low electric resistivity values ranged between $1 \Omega \text{ m}$ (VESes 5 and 35) and $20 \Omega \text{ m}$ (VESes 54 and 29) which corresponds to clay nature deposits.
- Uncompleted two geoelectric layers appear only in geoelectric cross section B–B'. The first layer is recorded beneath VESes 49, 48, 47, 5, and 6. It has relatively high resistivity

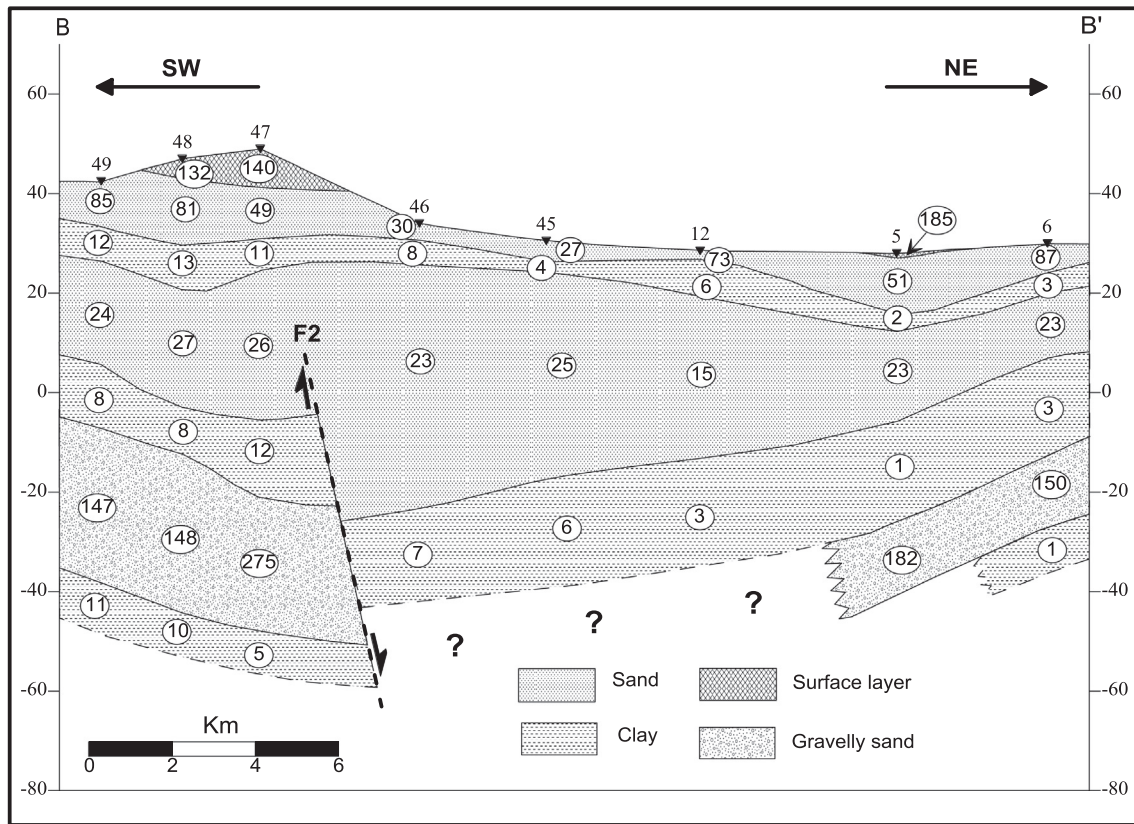


Figure 8 Geoelectric cross section B-B'.

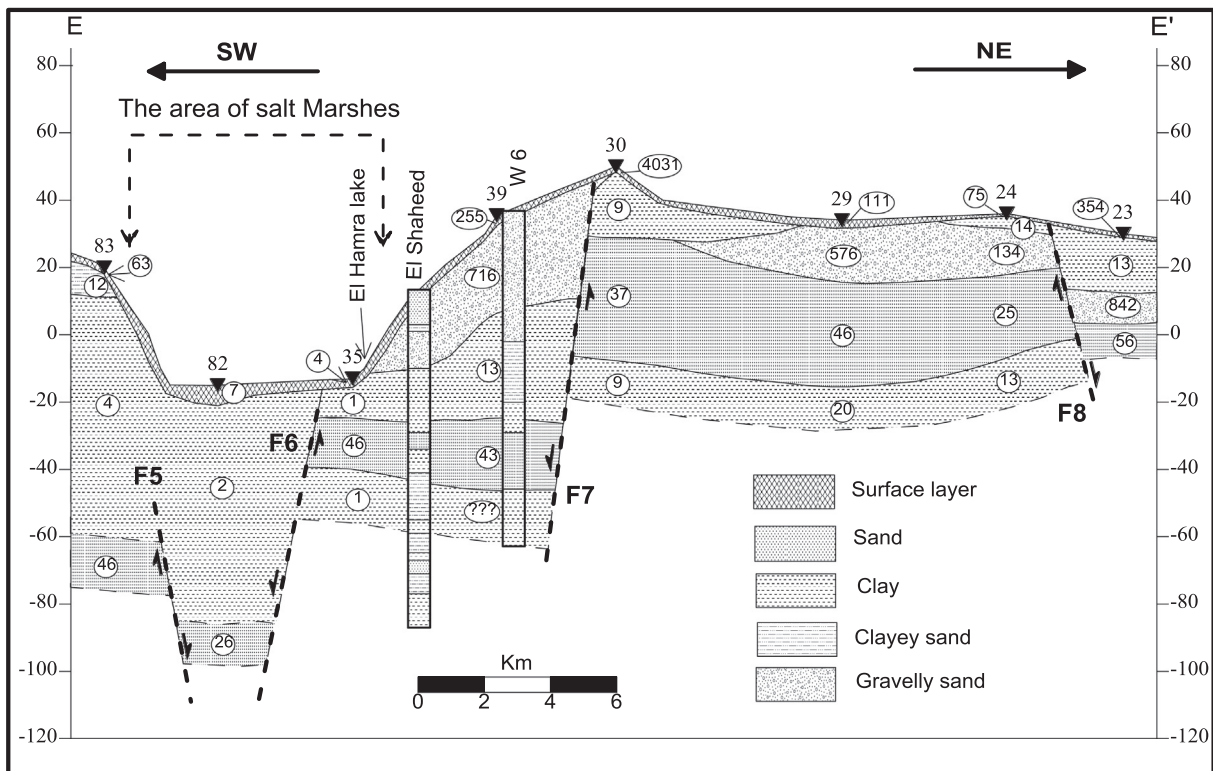


Figure 9 Geoelectric cross section E-E'.

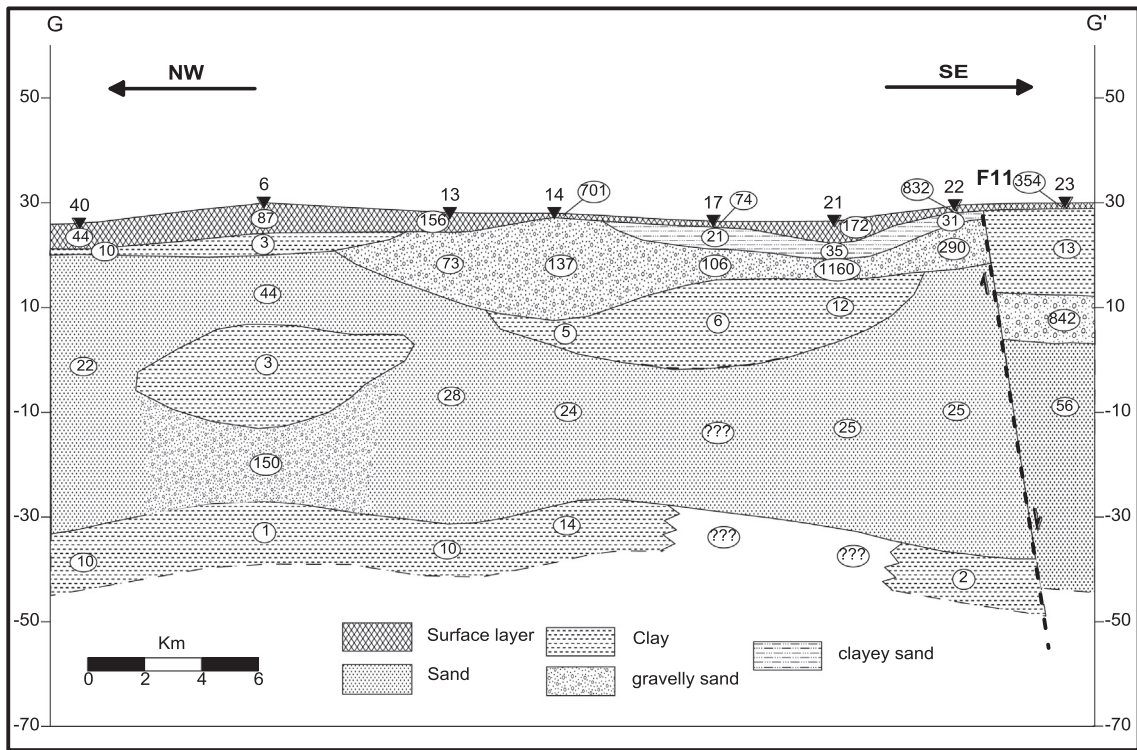


Figure 10 Geoelectric cross section G-G'.

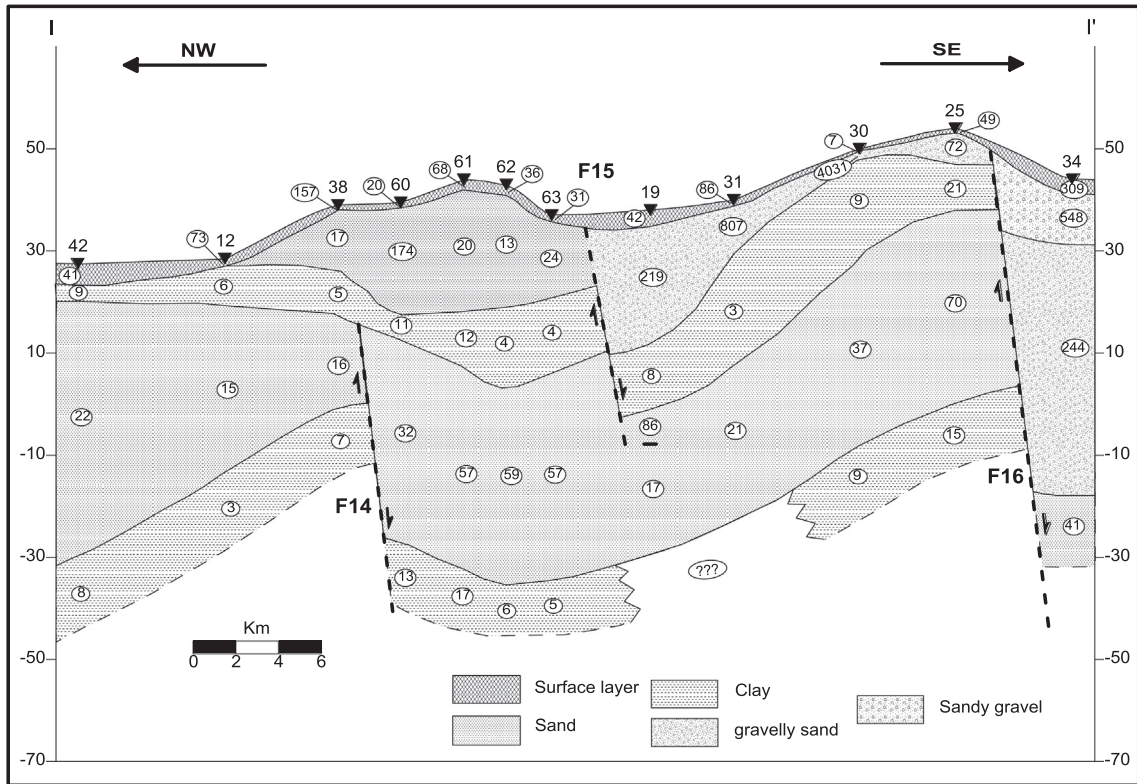


Figure 11 Geoelectric cross section I-I'.

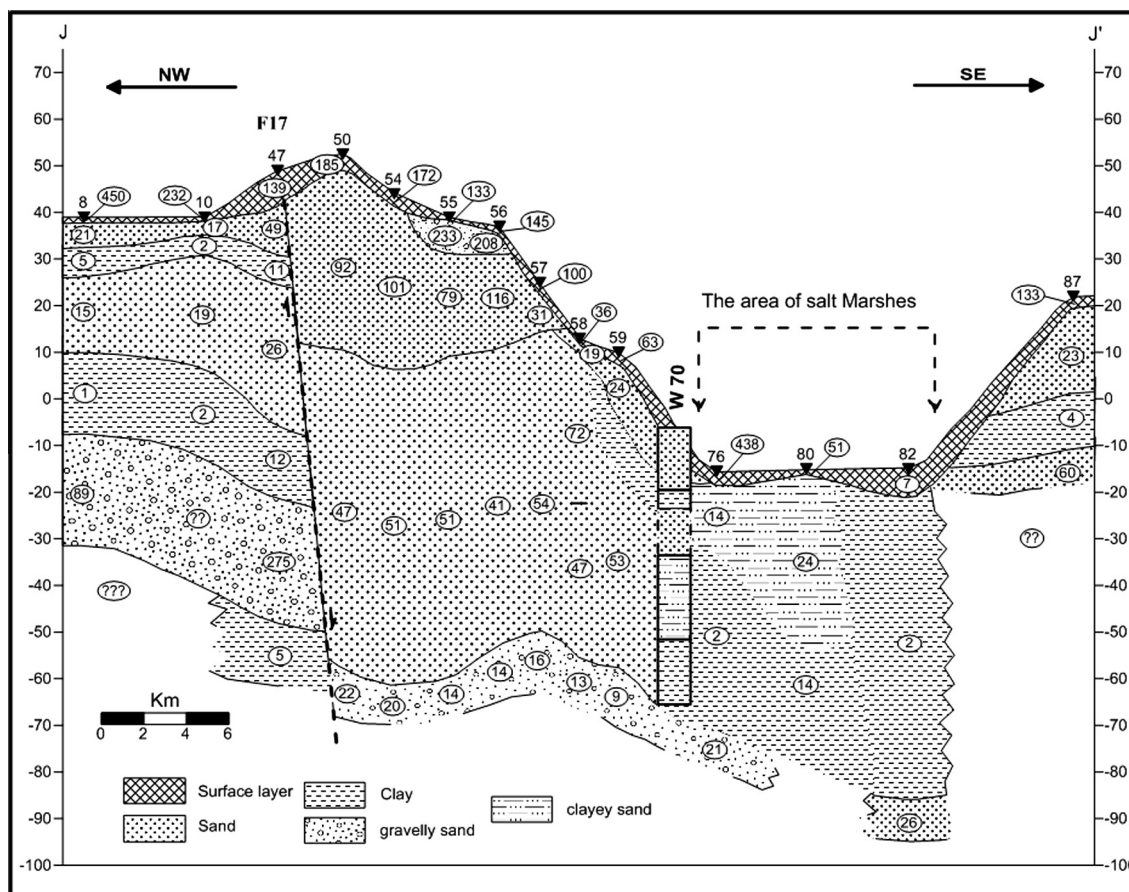


Figure 12 Geoelectric cross section J-J'.

values ranging from 147 to 275 Ω m, which reflects gravelly sand deposits. The thickness of this layer varies from 14 m beneath VES 6 and 32 m under VES 48 whereas the second geoelectric layer is determined below VESes 49, 48, 47, and 6. This layer has relatively low resistivity values varying from 1 to 11 Ω m which leads to a clay nature deposits.

4.3. Time domain electromagnetic (TDEM) survey

Electromagnetic methods have been extensively developed and adapted over the past three decades for the lateral and vertical mapping of resistivity variations (Kaufmann and Keller, 1983; Nabighian and Macanae, 1991).

In this study a set of 26 TEM stations were measured very close to the VES's sites (Fig. 13). A simple coincident loop configuration was employed (Fitterman and Stewart, 1986). The loop side length was 50 m. In all sites, the measurements were repeated up to five times. The best signal-to-noise data sets were chosen for further processing and interpretation. TDEM data were acquired using SIROTEM MK-3 Conductivity meter.

4.4. Interpretation of TEM data

Quantitative interpretation of TEM has been carried out using "IX1D software 2008". The models and the number of layers that resulted out from the interpretation of the nearby VES's are used as initial models to calculate the final models of TEM interpretation. In addition, during the interpretation, the resistivity values of the TEMs were constrained using the drilled boreholes nearby and were correlated with the lithology of these boreholes. Fig. 14 is a good example for the correlation procedure where the TEM 24 is correlated with the borehole W57. The interpreted geoelectric section shows slight difference from the lithological section.

The TEM stations that carried out in this area were used to construct three geoelectric cross sections oriented in NE-SW direction Figs. 15–17. The inspection of these geoelectric section shows that the study area can be differentiated into five geoelectric units according to their resistivity values:

- The first layer is a thin layer with resistivity ranging between 1 Ω m at (TEMs 8, 9 and 25) and 324 Ω m at (TEM 26). The great difference in the resistivity of this layer reflects

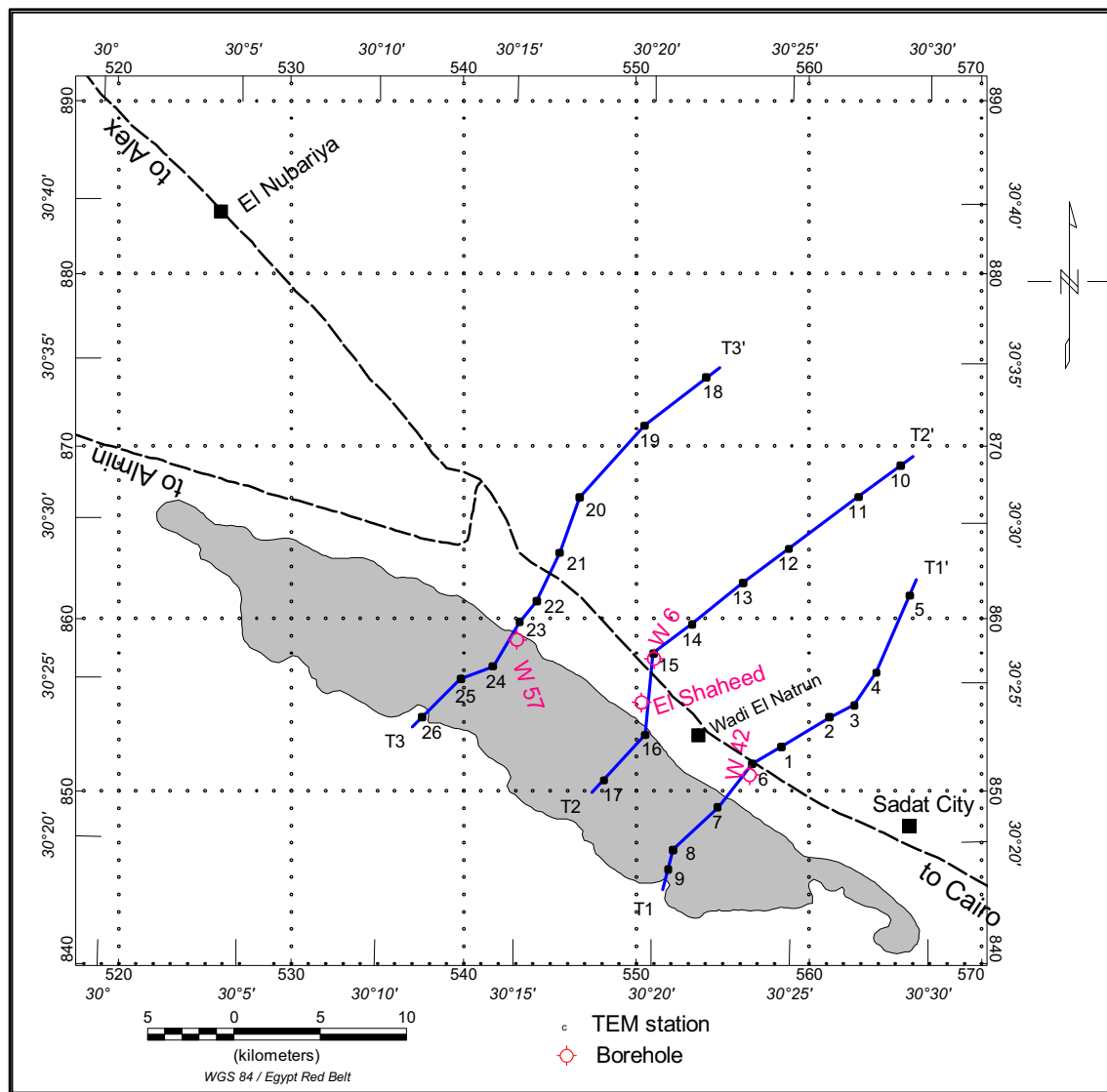


Figure 13 Location map for TEM stations and boreholes in the study area.

the inhomogeneity of the lithology, which corresponds to sands, silts, clay or gravels. The thickness of this layer ranges between 0.5 m and 2.8 m.

- The second layer has relatively moderate to high resistivity values ranging between $57 \Omega \text{ m}$ and $265 \Omega \text{ m}$ and represents the gravelly sand layer. The thickness of this layer ranges between 3.5 m at TEM 23 and 29 m at TEM 3.
- The third geoelectric layer has relatively low resistivity values ranging between $1 \Omega \text{ m}$ at TEM 17 and $27 \Omega \text{ m}$ at TEM 21 and is composed of clayey sand to clay deposits. It may represent the Pleistocene aquifer. In cross section T3–T3' (Fig. 17), this layer can be subdivided into three sub-layers from top to down: clay, clayey sand and clay deposits.
- The fourth geoelectric layer is implied by relatively moderate resistivity values varied from 15 to $59 \Omega \text{ m}$. These values reflect the presence of sand and gravelly sand deposits that

constitute the main Pliocene aquifer in the investigated area. The thickness varies from 9 m to 57 m.

- The fifth geoelectric layer has relatively low resistivity values ranging between 1 and $9 \Omega \text{ m}$ and is made up of clay. This layer is well correlated with boreholes w 6, w42 and w57.

5. Water aquifer parameters

Two maps for the depth to the main aquifer (Fig. 18) and its true resistivity (Fig. 19) are established depending on the results of the quantitative interpretation of the VES and TEM data. The depth to the main aquifer ranges from 6 at the northwestern portion near the Nubariya city to about 90 m at the southern parts where it increases to the south and southeast directions. The true resistivity of the aquifer

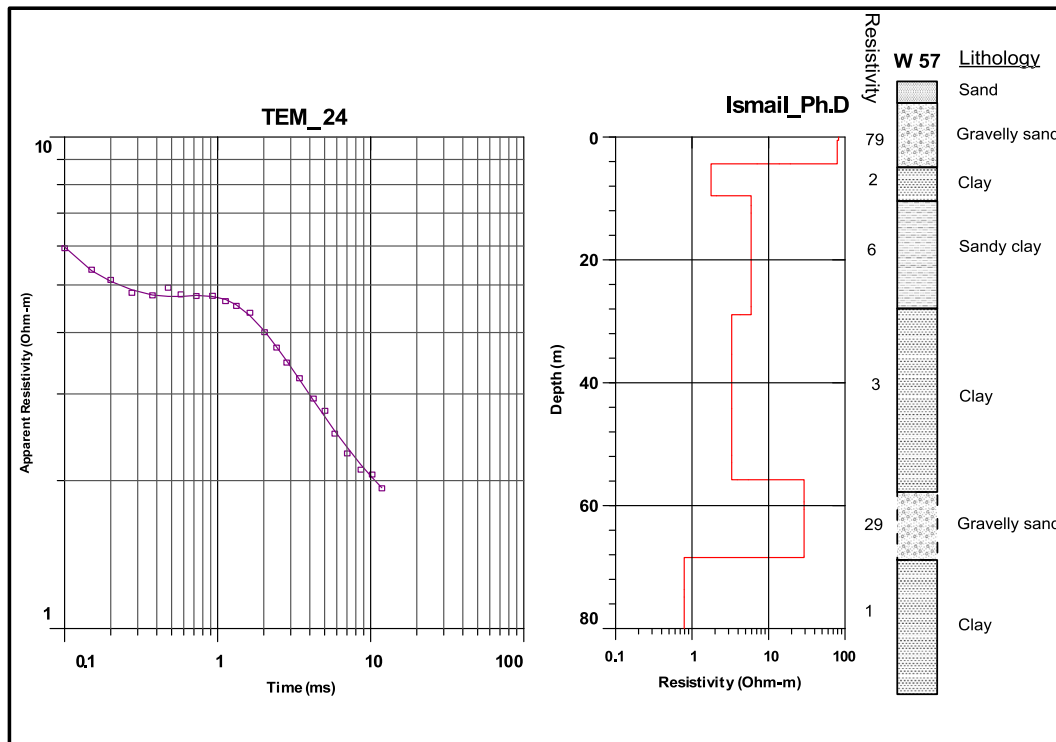


Figure 14 Lithology of well 57 and its corresponding interpreted geoelectric model of TEM24.

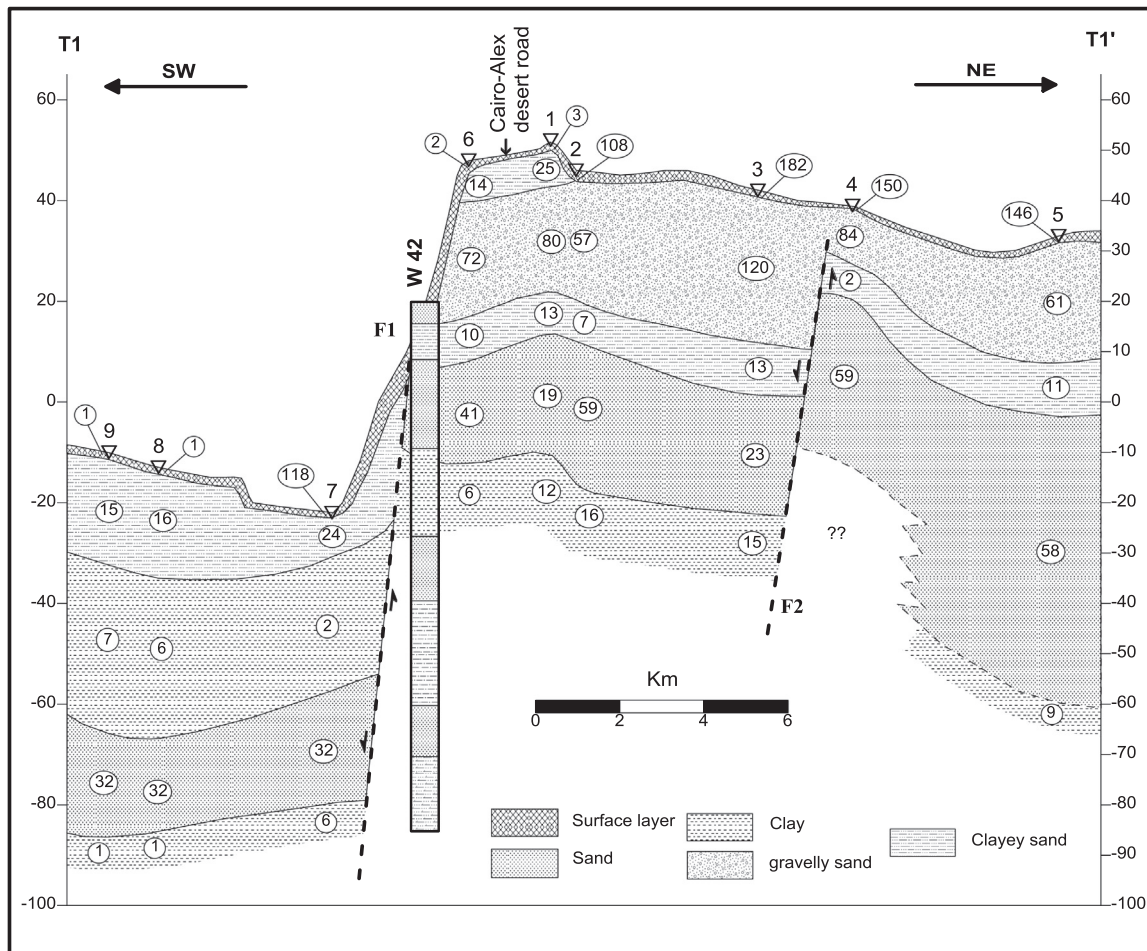


Figure 15 Geoelectric cross-section T1-T1'.

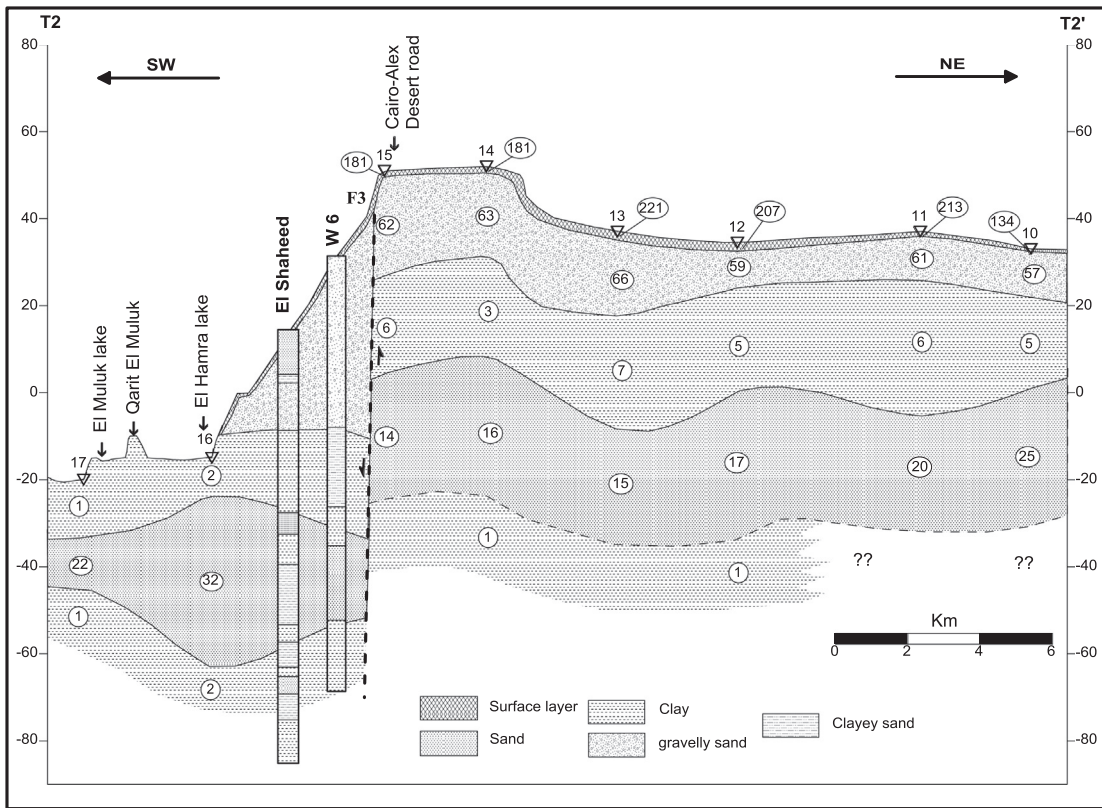


Figure 16 Geoelectric cross-section T2–T2'.

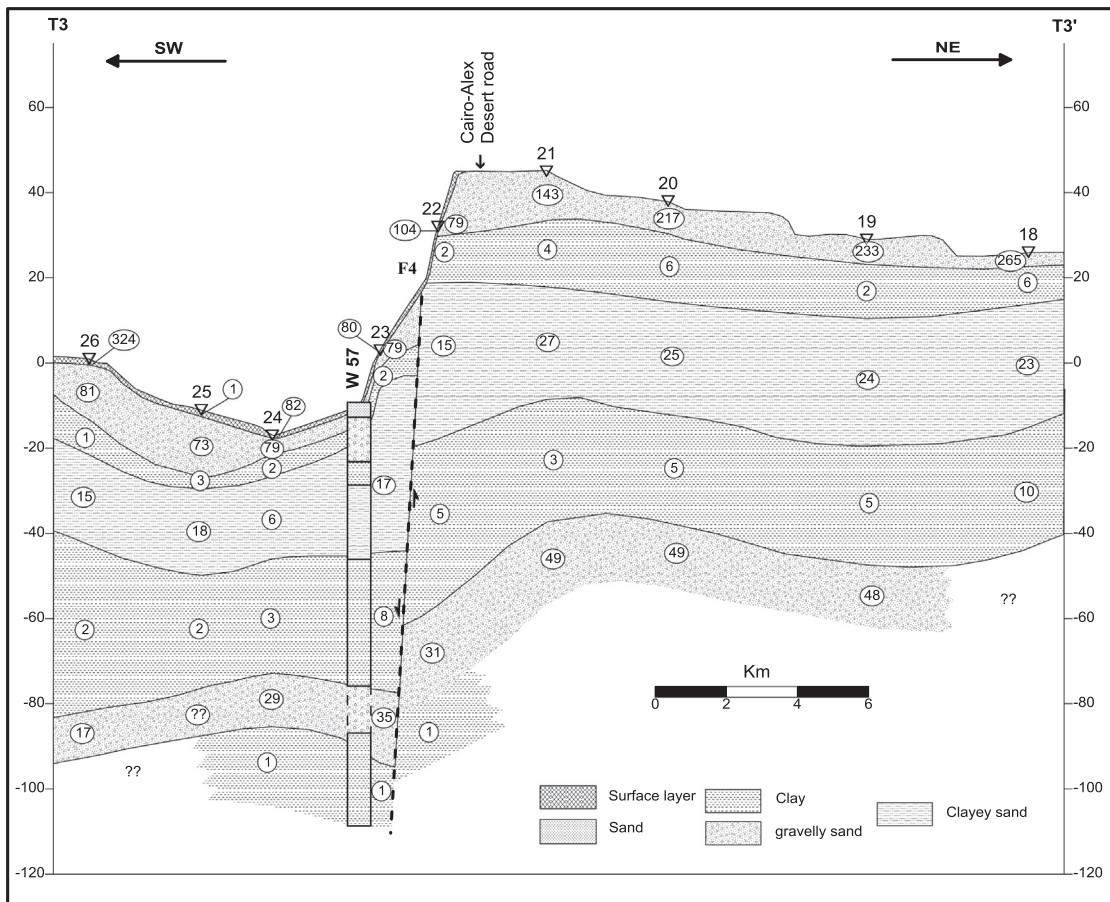


Figure 17 Geoelectric cross-section T3–T3'.

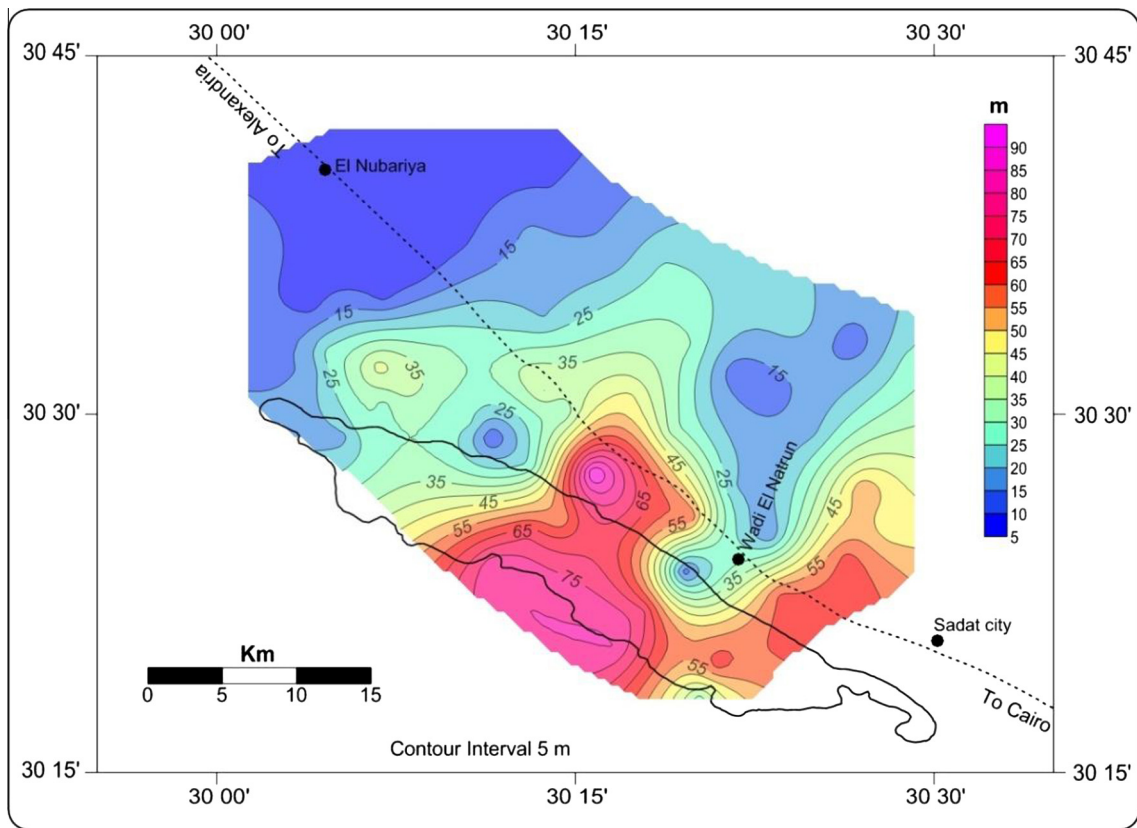


Figure 18 Depth map to the main aquifer in the study area.

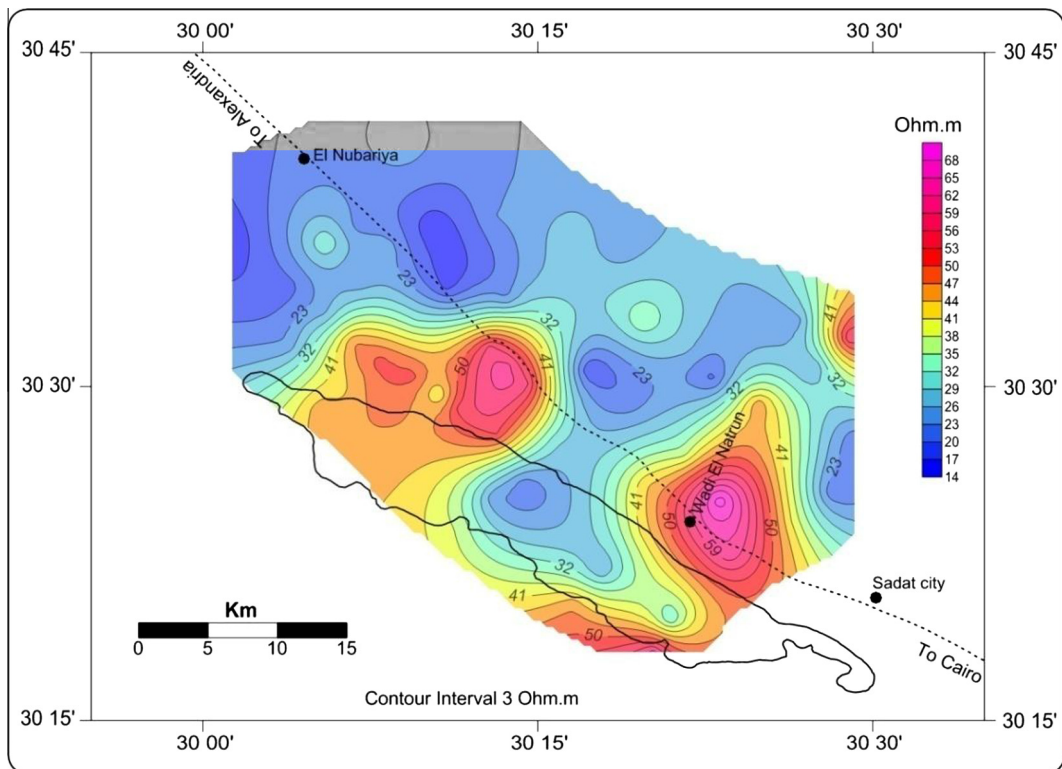


Figure 19 True resistivity map of the main aquifer in the study area.

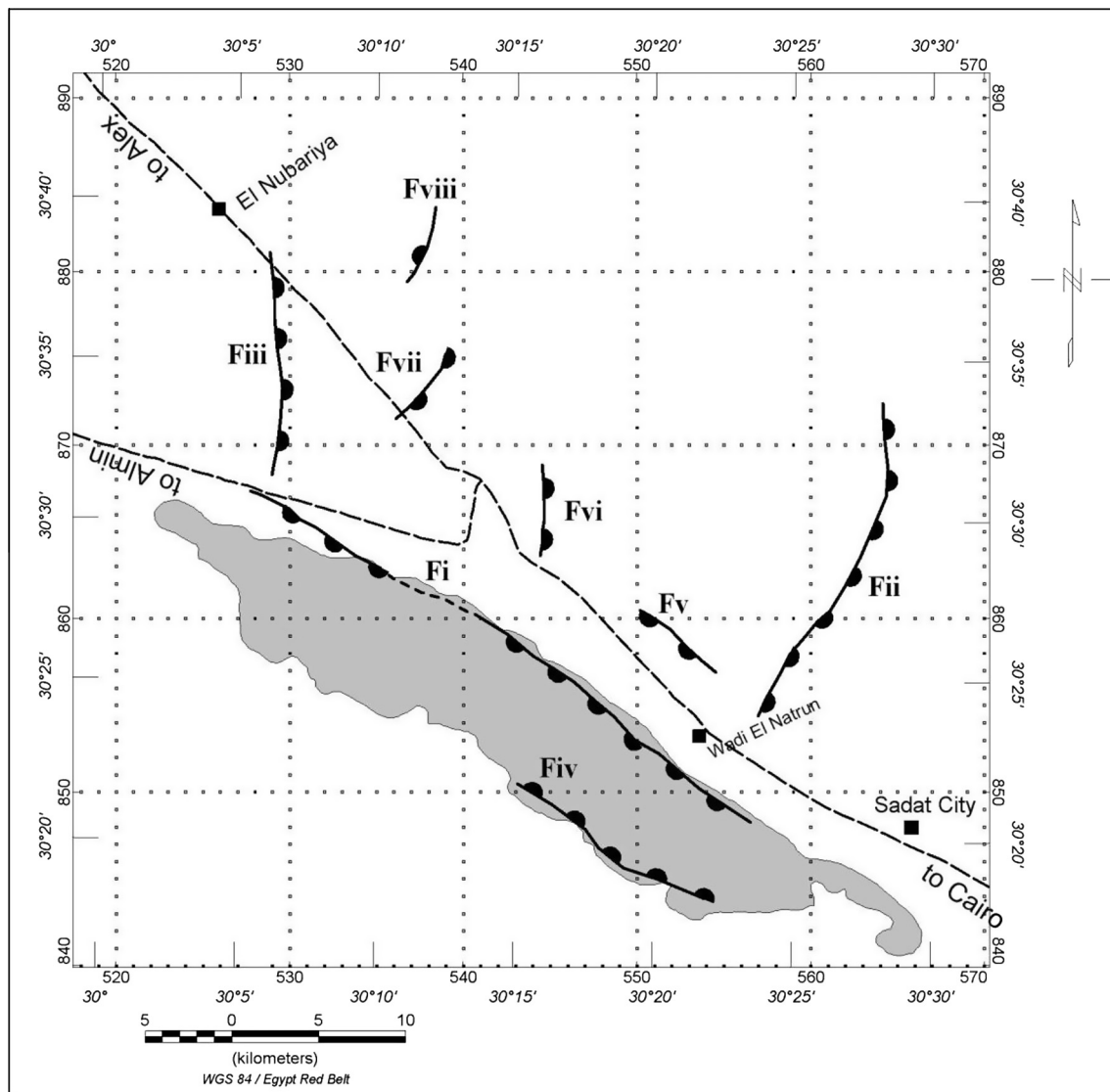


Figure 20 Deduced structure map based on the results of geoelectric interpretation.

varies from 15 to 70 Ω m. It decreases in the north and north-west direction whereas it increases in the central, southern and northeastern parts. The highest value is recorded near Wadi El Natrun city. A low value of resistivity can be detected in the area inside Wadi El Natrun valley. This aquifer is composed of sand or gravelly sand where the groundwater exists under confined conditions.

Generally the aquifer system in the area can be divided into Pleistocene and Pliocene aquifers. The Pleistocene aquifer is the shallower aquifer in the area and it almost consists of gravelly to clayey sand deposits. The Pliocene aquifer is the main aquifer where it is composed of sand to gravelly sand deposits.

Depending on the results of the geoelectric prospecting represented by the true resistivity map (Fig. 19), we can infer the quality of the groundwater. A brackish groundwater can be found at the northern and northeastern parts of the study area at shallow depths whereas relatively fresh water can be

detected at the southern and southeastern parts around Wadi El Natrun city at deep depths.

The inferred faults from the geoelectric sections are traced and collected to construct a structure map. This map (Fig. 20) shows the location and the throw of the interpreted faults in the study area. A major fault (Fi) passes parallel to the northeastern edge of Wadi El Natrun with a southwest throw. Another two important faults (Fii and Fiii) pass nearly perpendicular to Wadi El Natrun axis with thrown nearly to the east, in addition to five faults parallel or perpendicular to Alex-Cairo road. It is worth to mention that Wadi El Natrun and its lakes are structurally controlled by faulting systems trending NW direction.

6. Summary and conclusion

In this study, ninety three Vertical Electric Soundings (VES) and twenty-six TEM stations were used to define the

subsurface lithology and structures and to determine ground-water regime at El-Nubariya–Wadi El-Natrun area. Five geoelectric units reveal the subsurface sequence in the study area. The depth to the main aquifer ranges from 6 m at the northern part near El-Nubariya city to about 90 m at the southern parts where it increases to the south and southeast directions. Generally the aquifer system in the area can be divided into Pleistocene and Pliocene aquifers. A brackish groundwater can be found at the northern and northeastern parts of the study area at shallow depths whereas relatively fresh water can be detected at the southern and southeastern parts around Wadi El Natrun city at deep depths.

The area under investigation may be affected by a group of normal faults. The inferred faults from the geoelectric sections were traced and collected to construct a structure map. It is worth to mention that Wadi El Natrun and its lakes are structurally controlled by faulting systems trending NW direction.

Salt water of the lakes of Wadi El Natrun causes a serious problem especially for the agricultural proposes. That is why it is worthy to have a detail investigation to delineate the extension of the brackish water zone. To the north of the study area, especially near El-Nubariya city, a shallow clay layer at depth from 1.5 to 5 m causes a trapping for the surface water; this causes a very severe problem for the agriculture purpose in the area. We recommend installing a drainage system to overcome this problem.

Acknowledgments

The authors would like to thank Dr. Ahmed Mostafa Abd El-Gawad, Ain Shams University, for providing some of vertical electrical soundings. We are also indebted to the anonymous reviewers for their constructive comments.

References

- Abd El-Gawad, A.M.S., Ammar, A.I., 2004. The contribution of geoelectrical investigations in delineating the shallow aquifer in Wadi El Natrun area, Western Desert, Egypt. *EGS J.* 2 (1), 37–50.
- Abu El Ata, A.S.A., 1988. The relation between the local tectonics of Egypt and the plate tectonics of the surrounding regions using geophysical and geological data. In: *E.G.S. Proc. of 6th Ann. Meet.*, Cairo, Egypt, pp. 92–112.
- Abu El-Izz, M.S., 1971. *Landforms of Egypt*. The American Univ. Press, Cairo, pp. 128–154.
- Ahmed, F.M., Hassaneen, A.Gh., 1985. Interpretation of the anomalous geomagnetic field of Egypt with respect to the regional structural of Egypt. *NRIAG Bull. Ser. B V*, 101–126.
- CONCO, 1987. Geological map of Egypt 1: 500,000. Map Sheets NH36NW and NH35NE, CONCO with Cooperation of the Egyptian General Petroleum Corporation, Klitzsch, E., List, F. K., Pöhlmann, G. (Editors, Berlin), Cairo, Egypt.
- ElGalladi, A.A., Ghazala, H.H., Ibraheem, I.M., Ibrahim, El.Kh.H., 2009. Tectonic interpretation of gravity field data of west of Nile Delta region, Egypt. *NRIAG J. Astron. Geophys. Egypt*, 487–508 (special issue).
- El Shazly, E.M., 1977. The geology of Egyptian region. In: Nairn, A.E. M., Kaner, W.H., Stehli, F.G. (Eds.), . In: *The Ocean Basins and Margins*, vol. 4A. Plenum Press, pp. 379–444.
- El Shazly, E.M., Abdel-Hady, M., El Ghawaby, H., El Kassas, k., Khawasik, S.M., El Shazly, M.M., Sanad, S., 1975. Geologic Interpretation of Landsat Satellite Image for West Nile Delta Area, Egypt. The Remote Sensing Center, Academy of Scientific Research and Technology, Cairo, 38p.
- Embaby, A.A.A., 2003. Environmental Evaluation for Geomorphological Situation in Relation to the Water and Soil Resources of the Region North of the Sadat City, West Nile Delta, Egypt (Ph.D. thesis). Fac. Sci., Mansoura Univ., Mansoura, Egypt, 383p.
- Fitterman, D.V., Stewart, M.T., 1986. Transient electromagnetic sounding for groundwater. *Geophysics* 51 (4), 995–1005.
- Hefny, K., El Gandour, M.F.M., Khalil, J.B., Atta, S.A., 1991. Groundwater Assessment in Egypt. RIGW, Egypt.
- Idris, H., 1970. Groundwater investigation in Wadi El Natrun. In: *Proc. of IAEA Symposium, Beirut, Lebanon*, p. 26.
- Inman, J.R., 1975. Resistivity inversion with ridge regression. *Geophysics* 40, 798–817.
- Interpex Ltd., 2008. IX1D v3 Manual, 1-D DC Resistivity, IP, MT and EM Inversion Software, Golden, Colorado, USA. <<http://www.interpex.com>> .
- Kaufmann, A.A., Keller, G.V., 1983. In: *Frequency and Transient Sounding; Methods in Geochemistry and Geophysics*, vol. 16. Elsevier Publ., 685p.
- Keller, G.V., 1967. Application of resistivity methods in mineral and groundwater exploration program. In: *Mining and Groundwater Geophysics*. Geological Survey of Canada, No. 26, pp. 51–66.
- Khalil, A., Mansour, K., Rabeh, T., Basheer, A., Zaher, M.A., Ali, K., 2014. Geophysical evaluation for evidence of recharging the pleistocene aquifer at El-Nubariya Area, West Nile Delta, Egypt. *Int. J. Geosci.* 5, 324–340.
- Massoud, U., Kenawy, A., Ragab, El.-S., Abbas, A., El-Kosery, H., 2014. Characterization of the groundwater aquifers at El Sadat City by joint inversion of VES and TEM data. *NRIAG J. Astron. Geophys.* 3 (2), 137–149.
- Meshref, W.M., 1982. Regional structural setting of Northern Egypt. In: *6th E.G.P.C. Expl. Semin.*, Cairo, Egypt, 10p.
- Moody, J.D., 1973. Petroleum exploration aspects of wrench fault tectonics. *AAPG Bull.* 57, 449–476.
- Nabighian, M.N., Macanae, J.C., 1991. Time-domain electromagnetic prospecting methods. In: Nabighian, M.N. (Ed.), . In: *Electromagnetic Methods in Applied Geophysics*, vol. 2. Society of Exploration Geophysics, pp. 427–514.
- Riad, S., El-Etr, H.A., Makhles, A., 1981. Basement Tectonics of Northern Egypt as Interpreted from Gravity Data. *International Basement Tectonics Association Publication*, No. 4, pp. 209–220.
- Said, R., 1962. *The Geology of Egypt*. Elsevier, Amsterdam, New York, p. 377.
- Sallouma, M.K., Gomaa, M.A., 1997. Groundwater quality in the Miocene aquifer east and west of Nile Delta and in the north of the Western Desert, Egypt. *Ain Shams Sci. Bull.* 35, 47–72.
- Sandford, K.S., Arkell, W.J., 1939. In: *Paleolithic Man and Nile Valley in Lower Egypt*, vol. 36. Chicago Univ, Oriental Inst. Publ., pp. 1–105.
- Shata, A.A., 1953. New light on the structural development of the Western Desert of Egypt. *Bull. Inst. Desert d' Egypte T. III* (1), 101–106.
- Shata, A.A., 1955. An introductory note on the geology of northern portion of the Western Desert of Egypt. *Bull. Inst. Desert d' Egypte T. V* (1), 96–106.
- Shata, A.A., 1959. Geological problems related to the groundwater supply of some desert areas of Egypt. *Bull. Soc. Geogr. d' Egypte T. 32*, 247–262.
- Shata, A.A., El Fayoumi, I.F., 1967. Geomorphological and morphopedological aspects of the region west of the Nile Delta with special reference to Wadi El Natrun area. *Bull. Inst. Desert d'Egypte T. XIII* (1), 1–38.
- Shata, A.A., El Fayoumi, I.F., Tamer, M., 1970. *Geomorphology, Geology, Hydrology and Soils of Wadi El Natrun-Maryot Agriculture Project*. Pubi. Institute Desert.
- Shata, A.A., El Shazly, M.M., Attia, S.H., Aboul-Fetouh, M., 1978. The geology of the quaternary deposits and their natural relation to soil formations in the fringes west of the Nile Delta, Egypt. *Desert Inst. Bull.*, ARE 28 (1), 43–77.

- Shukri, N.M., 1954. Remarks on the geophysical structure of Egypt. Bull. Soc. Geogra., Egypt 27, 62–82.
- Tealeb, A., Abdel Rahman, E.M., 1985. Tectonic Trends in the Northern Part of the Western Desert of Egypt. Bull. Helwan Institute of Astronomy and Geophysics, No. 335.
- Yallouze, M., Knetsch, G., 1954. Linear structure in and around the Nile basin. Bull. Soc. Geogr., Egypt 27, 153–207.
- Youssef, M.I., 1968. Structural pattern of Egypt and its interpretation. AAPG Bull. 52 (4), 601–614.